ACADEMIC
PRESS

Temporal analysis of products: basic principles, applications, and theory

G.S. Yablonsky,[a] Maria Olea,[b,c] and G.B. Marin [c,*]

[a] *Department of Chemical Engineering, Washington University, I Brookings Drive, St. Louis, MO 63130, USA*
[b] *Department of Chemical Engineering, Babes-Bolyai University, Arany Janos 11, 3400 Cluj, Romania*
[c] *Laboratorium voor Petrochemische Techniek, Ghent University, Krijgslaan 281 S5, 9000 Ghent, Belgium*

Abstract

This paper discusses a temporal analysis of products approach, which can be considered as an advanced kinetic strategy at the boundary between traditional applied kinetics and surface science. The basic principles, examples of application in heterogeneous catalysis and theoretical framework are discussed.
© 2003 Elsevier Science (USA). All rights reserved.

Keywords: TAP; Transient; Kinetics; Modeling

1. Introduction

The temporal analysis of products (TAP) reactor system is an important new tool for investigating "gas–solid" reactions, particularly reactions on industrial catalysts. Originally created by John T. Gleaves in 1988 [1] and later modified by him in 1997 [2], the TAP technique found an application in many areas of chemical kinetics and chemical engineering [3–12], especially due to its submillisecond time resolution. This is accomplished by injecting an extremely narrow gas pulse into one end of a microreactor and continuously evacuating the other end. The time resolution of a TAP experiment can be controlled by shortening the reactor bed length and by reducing the width of the initial gas pulse. Two advantages can be attributed to the operation in high vacuum. The first is that external mass transfer limitations are completely absent. The second is that gas transport through the catalyst bed is governed by Knudsen diffusion. In this case, the diffusivities of the individual component of a gas mixture are independent of pressure, concentration, or the composition of the gas mixture. Moreover, performing transient response experiments in the limit of Knudsen diffusion minimizes collisions between gas-phase molecules so that the transient response of product molecules in the TAP system is a measure of gas–solid interactions.

To characterize these gas–solid interactions and to reveal the complex mechanism of catalytic reactions two types of experiments are performed in the TAP system.

The first type is a so-called *state-defining* experiment in which the catalyst composition is not significantly perturbed by a pulse of small intensity. The pulse intensity must guarantee the Knudsen diffusion regime; i.e., the transport must remain well defined. State-defining experiments provide kinetic parameters corresponding to a given state of the catalyst; e.g., in the case of the irreversible transformation of a hydrocarbon on a metal oxide catalyst the corresponding kinetic coefficient depends on the state of the metal oxide surface and in particular on the oxidation state. In the so-called "pump-probe" experiment a single pulse of one substance, say a reducing reactant, is admitted followed by a single pulse of another substance, say an oxidizing agent. By varying the delay between the two single pulses and the frequency of repeating the cycle, information on the lifetime and reactivity of the adsorbed species is obtained. These species are created during the first single pulse and probed during the second single pulse. The yield of each product is a measure of the amount of adsorbed precursor present at the time of the pulse. By plotting the various product yields as a function of the delay interval between the pulses, the lifetime of the various adspecies can be determined.

The second type of TAP experiment is a *state-altering* experiment that changes the catalyst composition in some predetermined fashion. In multipulse experiments, a large number of pulses is injected, and reactant and product

* Corresponding author.
 E-mail address: guy.marin@rug.ac.be (G.B. Marin).

responses are monitored. By performing TAP multipulse experiments, the interaction of a component with the surface at different catalyst compositions can be studied.

State-defining and state-altering experiments can be performed in sequence. In the so-called *interrogative cycle* the given state of catalyst is probed using state-defining experiments involving different substances (O_2, hydrocarbons, CO, etc.). Next, a state-altering experiment is performed resulting in a new catalyst state. This state is tested again by different substances in state-defining experiments.

This approach was defined by Gleaves and Yablonsky as interrogative kinetics (IK) [2]. IK attempts to systematically probe a variety of different catalyst states, and to understand how one state evolves into another.

2. Description and operation of a TAP reactor system

The TAP reactor system was originally created to assist catalyst development and characterization at Monsanto [1]. Later, a new improved apparatus, called TAP-2 reactor system, has been developed [2], aimed at extracting kinetic information from a heterogeneous catalytic system and revealing mechanisms of complex heterogeneous catalytic reactions. The critical difference between TAP and TAP-2 reactor systems is the positioning of the microreactor and

the detector that measures the reactor effluent. In the TAP-2 system, the two devices are physically much closer, and as a result the detection efficiency of the TAP-2 system is much higher.

The TAP-2 reactor system can be used to perform transient as well as steady-state experiments at pressures ranging from 10^{-7} to 250 kPa, and temperatures ranging from 200 to 1200 K. However, the specific features of the TAP systems are exhibited in the Knudsen domain in the course of vacuum transient experiments. As already mentioned, pulse intensities in vacuum experiments range from 10^{13} to 10^{17} molecules/pulse, with a pulse width of 250 µs, and a pulse frequency between 0.1 and 50 pulses/s. Such time resolution characteristics are unique among other kinetic methods. Possible experiments include high-speed pulsing, both single pulse and multipulse response, steady-state isotopic transient kinetic analysis (SSITKA), TPD, and TPR. A schematic overview of a TAP reactor system is shown in Fig. 1.

In a typical pulsed mode experiment, the pulse mixture contains reactants and an inert gas as internal standard. Consequently, responses, exit flow time dependencies, for reactants, products, and inert are monitored. For a typical experimental set-up only one gaseous component can be measured during one pulse. When more than one substance is of interest, the single-pulse TAP experiments must be
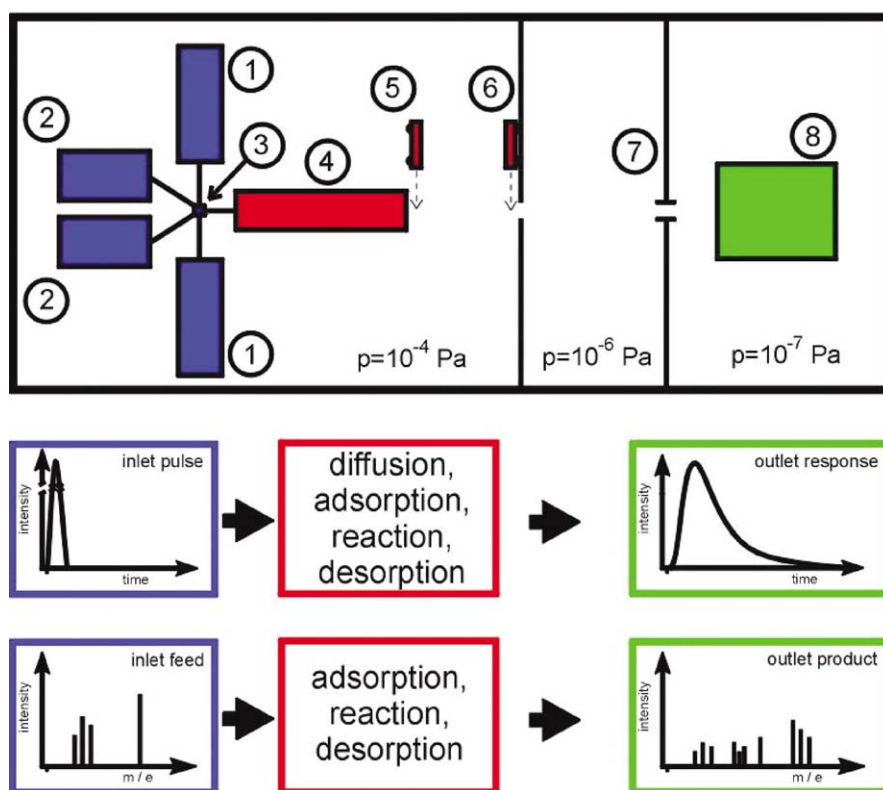

Fig. 1. Schematic diagram of the TAP reactor depicting the movement of a gas pulse from the microreactor to the quadrupole mass spectrometer. (1) High-speed beam valve, (2) continuous flow valve, (3) zero-volume manifold, (4) catalytic microreactor, (5), (6) cryo shields (all of these being situated in the reactor chamber), (7) differential chamber, (8) detector chamber.
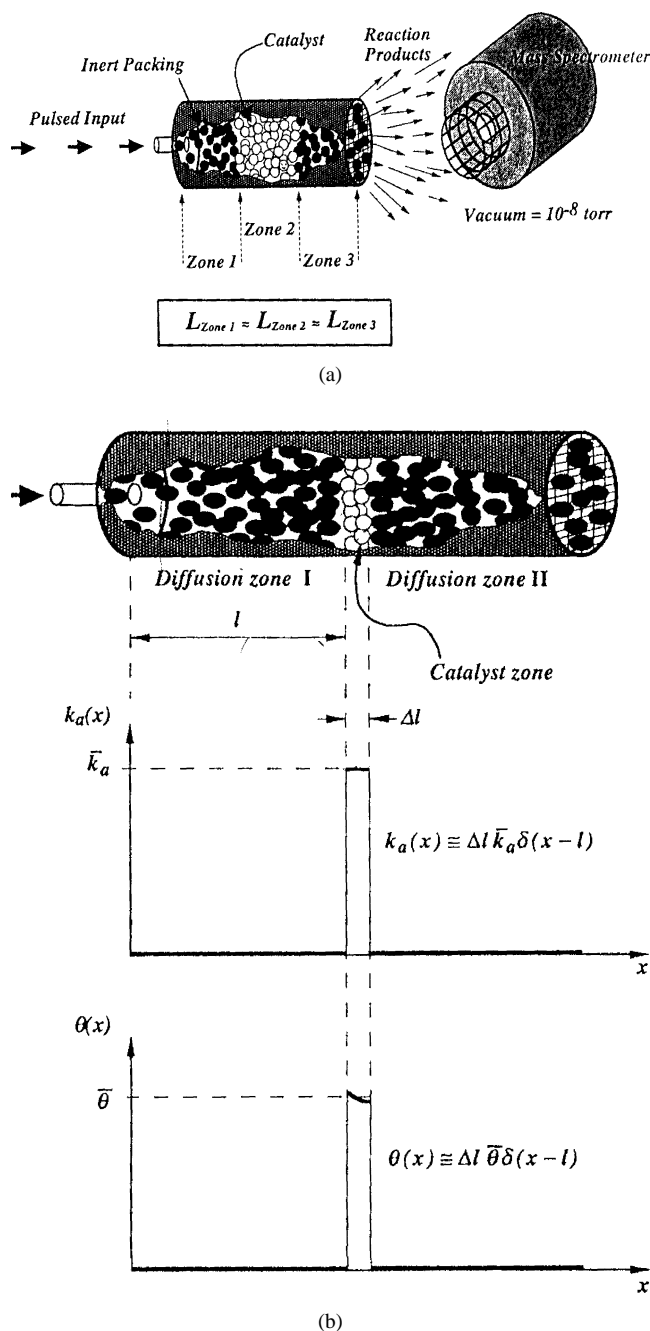
Fig. 2. (a) Three-zone reactor with QMS [13]. (b) Thin-zone reactor and dependencies of k_a and θ on the axial coordinate x [13].

repeated. To provide simultaneous multisubstance measurements, the multitrack system has been introduced [4]. In this system, the gas leaving the reactor can be analyzed for three components using three mass spectrometers in line.

The TAP microreactor configuration which is the most commonly used, is the so-called "three-zone" configuration (Fig. 2a). The TAP microreactor can be packed with catalyst and inert particles. The catalyst zone is sandwiched between two beds of inert particles, called inert zones. The main advantage of the three-zone TAP reactor is that the catalyst zone can be more easily maintained under isothermal con-

ditions. However, it is difficult to maintain a uniform profile of the surface catalyst composition because of the gas concentration gradient, which is the driving force of diffusional transport. In multipulse experiments, the nonuniformity of the catalyst composition becomes significant.

Recently, a "thin-zone" configuration was proposed by Shekhtman et al. [13] (Fig. 2b). In a thin-zone reactor, the thickness of the catalyst zone is made very small compared to the whole length of the reactor. Then, the change of gaseous concentration across the thin catalyst zone can be neglected, and the catalyst composition can be considered as uniform. In the thin-zone approach it is possible to separate the diffusional process from the chemical reaction. Uniformity of catalyst composition and model simplicity make the thin-zone TAP reactor configuration very useful.

3. Basic principles of TAP

The basic principles of TAP follow:

1. Well-defined Knudsen diffusion as a "measuring stick" for chemical reaction characterization.
2. Insignificant change of the solid material during a single pulse experiment.
3. Uniformity of the surface composition of the material across the active zone.

The first and the second principles were reported in the pioneering paper of 1988 [1]. Later, these principles have been developed in more detail. The necessity of the active material uniformity was first stressed in a paper devoted to the thin-zone TAP reactor in 1999 [13].

3.1. Knudsen diffusion as a "measuring stick"

A common approach for extracting kinetic information is to measure the rate of chemical reaction using the rate of mass transport as a "measuring stick." Transport, however, is a complex process that involves both diffusion and convection and can be different in different parts of a catalytic system. Consequently, special experimental strategies have been developed to distinguish kinetic information from transport phenomena. In traditional steady-state experiments, convectional transport that is supposed to be well defined provides a measuring stick and diffusional transport neglected. In contrast, in a typical TAP experiment, the diffusion, particularly Knudsen diffusion, is the only transport mechanism, which obviously must not be eliminated.

In the Knudsen diffusion regime, the diffusivity is determined by [14]:

$$D_e = \frac{\varepsilon_b}{\tau} \frac{d_i}{3} \sqrt{\frac{8RT}{\pi M}}, \qquad d_i = \frac{4\varepsilon_b}{3(1 - \varepsilon_b)} r_p. \qquad (1)$$

Thus, in the Knudsen regime, the transport of individual species is independent on the gas composition and the

mass transport is well defined. In TAP experiments, the purely diffusional transport serves as a specific "ruler" to extract kinetic information. The exit flow is described by the standard diffusion curve when only diffusion occurs. In the "reaction–diffusion" case, the exit flow is changed, and this change is attributed to the reaction.

3.2. Insignificant change of the solid material during the pulse experiment

With the TAP-2 system, a typical Knudsen pulse contains 10^{13} molecules or 10^{-10} moles. Assuming that a catalyst sample has a surface area of 10 m^2/g, a single pulse would be equivalent to 10^{-6} of the total surface area of 0.1 g sample. If the active surface area of the catalyst comprises a reasonable fraction (e.g., $\geqslant 0.1\%$) of the total surface area of the catalyst, then a single pulse will have a negligible effect on the active surface. Whenever the number of reactant molecules in a pulse is significantly smaller than the number of active sites of the catalyst, the catalytic system remains in the same state after the measurement, justifying the term "state-defining experiment."

3.3. Uniformity of the surface composition across the active zone

This principle has to be considered as absolutely necessary in TAP studies because kinetic information corresponding to a given catalyst composition cannot be obtained directly when nonuniform catalyst states are probed.

4. The place of the TAP experimental method among other kinetic methods

Kinetic studies focus on the selection of an adequate rate expression and determination of the unknown rate parameters it contains. To obtain this information, steady-state and/or transient experiments can be performed. Transient experiments provide information that cannot be obtained from steady-state experiments. While steady-state experiments give a global picture of the reaction kinetics, transient experiments give information relative to the individual steps involved. Being a transient technique, the TAP method uses an experimental strategy different from other nonsteady-state techniques. To illustrate the differences, a comparison of these techniques can be made by discussing the following issues:

1. Uniformity of the active zone.
2. Domain of conditions.
3. Possibility to obtain relevant kinetic information.
4. Correspondence between observed kinetic characteristics and catalyst properties.
5. Model-free data interpretation for determining kinetic data (rate of reaction, yield, selectivity, etc.).

The comparison will be primarily focused on the conceptual features. TAP will be compared with continuous stirred tank reactors (CSTR) and plug flow reactors (PFR) without going into the detailed implementation of these two reactors.

4.1. Uniformity of the active zone

4.1.1. CSTR
Until today, there was an indisputable belief that a CSTR can minimize the concentration gradients within the reactor. Now, under influence of computational fluid dynamics (CFD), this belief was suppressed by uncertainty, especially in the case where more than one fluid phase is involved. Obviously, it is possible to calculate stirred tank reactors [15] using CFD methods. However, there are many uncertainties in the description of the relevant transport phenomena. In fact, the rigorous theory of CSTR that would allow us to clearly understand its hydrodynamic and mathematical status (e.g., based on the idea of averaging) has not been developed yet. The domain of conditions that provides perfect mixing on both macro- and microscale has not been identified either.

4.1.2. PFR
In a PFR, the concentration gradients in the radial direction can be neglected. However, there is an essential concentration gradient in the axial direction, and, hence, a corresponding axial nonuniformity of the catalyst composition.

4.1.3. TAP
The original configurations of a TAP reactor, such as the three-zone configuration, were characterized by a nonuniform catalyst composition across the catalyst bed similar to a PFR. The thin-zone configuration, discussed earlier, does not have such a drawback.

There is a difference between the roles of diffusion and convection in a CSTR compared to TAP. The diffusion is always present as a special phenomenon in all experiments involving mass transport. In a CSTR, the disturbing effect of diffusion on the observed characteristics is minimized; diffusion is not eliminated but complemented by stirring. In TAP experiments, convection is easily and completely eliminated, and diffusion is well defined.

4.2. Domain of conditions

CSTR and PFR reactors provide data obtained under temperature and pressure conditions which are close to the industrial conditions. For highly exothermic reactions, a CSTR often operates under low conversions to maintain an isothermal regime.

As for the TAP system, it may operate in a wide domain of working conditions. However, the most appropriate TAP regime (Knudsen regime), in which the transport is well defined, is located within 10^{-2}–10^{-1} Pa. Such a domain is at the upper boundary of the "surface science" domain. TAP

experiments make a bridge between surface science applied in heterogeneous catalysis and traditional applied kinetics. Thus, the well-known "pressure gap" between these two areas is now reduced, but not eliminated.

4.3. Possibility to obtain relevant kinetic information

Both devices, CSTR and PFR, are mostly used to obtain steady-state kinetic information. Steady-state kinetic dependencies are usually related to the rate-determining step(s) of a complex catalytic process and do not provide detailed information related to the individual steps. To characterize individual steps, nonsteady-state experiments are required.

In heterogeneous catalysis, the idea of conducting nonsteady-state kinetic experiments in a CSTR was proposed more than 30 years ago by Bennett [16]. Nonsteady-state CSTR can be simulated via ordinary differential equations and even analytical solutions can be obtained sometimes. As for the nonsteady-state regime in the PFR, it can be simulated using integrating partial differential equations (PDEs). Today, this difference no longer makes nonsteady-state CSTR experiments preferable taking into account an increase in computing power and availability of efficient easy-to-use algorithms. Moreover, according to Bennett [6], there is a serious experimental drawback in using CSTR reactors for transient experiments. In many cases, these reactors have a "dead volume" inside or outside which influences the transient behavior. Bennett even concludes that "in some cases it is no longer advantageous to do experiments in an ideal mixed-flow reactor (CSTR)." In the 1970s, Kobayashi and Kobayashi [17] proposed an efficient "transient response method" based on the differential PFR. Generally, a PFR can provide rich information using the step response or wavefront propagation experiments. However, the PFR time resolution is limited by the imposed step function of the reactant concentration in the carrier gas and is much lower than that of the TAP technique. In TAP experiments, it is possible to study fast catalytic reactions with relaxation times as short as 10^{-4}–10^{-3} s.

4.4. Correspondence between observed kinetic characteristics and catalyst properties

In a typical CSTR or PFR experiment, there is no tool or procedure for monitoring the catalyst composition. In situ catalyst characterization by spectroscopic techniques does not always provide unambiguous information about the important surface species. As result, using CSTR or PFR data, for both steady-state and nonsteady-state cases, it is difficult to directly relate the observed kinetic characteristics to the material properties. Changes of the catalytic material during the reaction make the determination of such relationships even more challenging.

Some other techniques such as an isotopic step response experiment allow us to determine the amount of surface

intermediates (the number of "working active sites") by a so-called steady-state isotopic transient kinetic analysis. This approach was proposed by Happel et al. [18], and developed by Bennett [19], Bilouen [20], and Shannon and Goodwin [21]. It is based on the determination of isotopic labels in the reactor effluent species versus time following a stepwise change in the isotopic labeling of one of the reactant species in the reactor feed. SSITKA data can be used to determine the amount of surface substances as well as the rates of their formation characterizing the given steady-state of the catalyst. Steady-state isotopic transient experiments could be performed in CSTR or PFR reactors. However, experimental data obtained from a "CSTR–SSITKA" combination have a large limitation because of the experimental errors in isotope step response experiments (see the explanation by Shannon and Goodwin [21]). The common procedure in SSITKA application is a combination of the PFR with the SSITKA approach. At the same time, PFR data are shadowed by the catalyst nonuniformity.

The interrogative kinetics approach in the TAP studies gives a way to reduce the pressure gap between the Knudsen regime and normal condition domains. In TAP experiments under Knudsen diffusion conditions many kinetic characteristics of complex catalytic materials can be obtained as a function of surface concentrations that do not change (or do not change significantly) during the kinetic characterization. It is reasonable to consider that these parameters will be independent of the gaseous composition in a wide pressure domain. Moreover the detailed analysis of transient TAP characteristics of gaseous substances (especially, time delays) may provide information about the surface intermediates and their kinetic parameters that can be expanded to the normal conditions. A new theoretical framework for extracting this information will be presented in Shekhtman et al. (submitted for publication). However, observing short-lived intermediates and corresponding kinetic characteristics under normal conditions is still a large challenge.

4.5. Model-free data interpretation

Ideally, kinetic information should be extracted in a model-free manner. This means that during the experimental procedure and the following data analysis, no bias is introduced by presuppositions about the form of the kinetic dependencies, detailed mechanisms, reactor models, etc.

In terms of reactor model, the analysis of steady-state CSTR experimental data can be considered to be model-free. For the steady-state case, the consumption rate of a reactant, R, follows from

$$R(c) = \frac{F_v(c^0 - c)}{V_{cat}}. \tag{2}$$

For a nonsteady-state CSTR, the consumption rate follows from a mass balance for the reactant including an accumula-

Table 1
The place of TAP approach among other kinetic approaches

Approaches	Uniformity of catalyst composition	Domain of conditions	Reliability of the information	Control of gaseous substance amounts stored/released by catalyst	Model-free or not
CSTR	Typically, it is assumed for the steady-state case	Normal conditions, industrial domain	Steady-state information is reliable; nonsteady-state information is not	No	Steady-state CSTR is model-free. CSTR + SSITKA is model-free. Nonsteady-state CSTR gives rise to errors.
PFR	No uniformity	Idem as CSTR	Both steady-state and non-steady-state information are reliable.	No	Steady-state PFR is model-free. Nonsteady-state PFR is not model-free.
TAP reactor	No uniformity (three-zone configuration)	The top of the "surface science" domain	Nonsteady-state information is reliable.	Yes, especially for the thin-zone TAP reactor	The first modifications of TAP reactor are not model-free.
	Uniform (thin-zone configuration)				The thin-zone TAP reactor gives model-free information using Y-procedure.

tion term:

$$R(c) = \frac{V_g}{V_{cat}} \frac{dc}{dt} - \frac{F_v(c^0 - c)}{V_{cat}}. \tag{3}$$

If the derivative, dc/dt, is experimentally known, $R(c)$ can be obtained and the procedure is model-free. However, in practice, the determination of dc/dt gives rise to errors.

For the steady-state PFR, the reaction rate can be determined in a model-free manner by taking the derivatives from the experimental dependencies "conversion versus space time." This is known as the differential method of PFR data analysis. As for the nonsteady-state PFR, to extract reaction parameters, a model, which is a set of partial differential equations, has to be solved analytically or numerically. The integration along the axial reactor coordinate requires some assumptions about the kinetic model and, hence, about the detailed mechanism of reaction. Therefore, such data analysis is definitely not a model-free procedure. An application of the differential method to nonsteady state PFR data is extremely difficult because of experimental errors, just as in the case of CSTR.

A combination of CSTR and SSITKA approaches must provide model-free information about the number of working active sites, which is not true for a combination of PFR and SSITKA approaches because a PFR model is always needed.

As for the TAP method, the first configurations of the TAP reactor (three- and one-zone TAP reactors) could not provide model-free kinetic information either. The obtained data needed to be described based on assumed models. Recently [22], a general expression for primary characterization of catalyst activity using a TAP single pulse experiment was derived as

$$1 - X = \frac{1}{\cosh(\Psi) + \alpha\Psi\sin(\Psi)}, \tag{4}$$

where Ψ is the reaction–diffusion parameter,

$$\Psi = \sqrt{\varepsilon_b \frac{(\Delta L)^2}{D_{g,cat}} k_{app}},$$

and α is the diffusional–geometrical parameter,

$$\alpha = \frac{D_{g,cat}}{D_{g,in}} \frac{l_3}{l_{cat}}.$$

In a typical case,

$$\frac{D_{g,cat}}{D_{g,in}} = 1.$$

Expression (4) was obtained for the three-zone TAP reactor, the most commonly used TAP reactor configuration, on the basis of the corresponding model presented below.

A new theoretical method developed for the thin-zone TAP reactor, called the Y procedure [23], allows us to obtain values of reaction rates and, hence, kinetic parameters directly from exit flow data without any assumption regarding the detailed kinetic model. The Y procedure is briefly described below. Table 1 summarizes the place of the TAP approach among other kinetic approaches.

5. TAP data analysis

The TAP experiment can provide two kinds of information about a reaction: qualitative and quantitative information.

Qualitative information allows us to obtain insight into the reaction mechanism. As mentioned earlier, using the TAP experiment, it is possible to detect short-lived intermediate substances that are released by the catalyst surface into the gas phase and, then, reveal information about various elementary steps of the complex catalytic reaction. To obtain qualitative information, single-pulse, pump-probe, and multipulse TAP experiments can be used. Examples presented

below will illustrate the capability of the TAP experiment in this respect.

5.1. Single-pulse TAP experiments

The conversion of methanol to light olefins over a H-ZSM-5 zeolite was studied by means of temporal analysis of products, performing mainly single-pulse TAP experiments [24]. A methanol pulse train was injected and the response of the products, namely olefins (especially propylene), water, dimethyl ether, formaldehyde, and methane was recorded and compared with the methanol response (Fig. 3). It can be seen from Fig. 3a that the methanol response is very broad indicating that methanol adsorbs reversibly on the catalyst. The water response is about as broad as the methanol response. This suggests that water is rapidly produced from methanol. The dimethyl ether response and the olefin responses were strongly broadened. All olefin responses have the same shape (see Fig. 3b). The formaldehyde and methane responses are not much broadened, showing that both products are rapidly produced from methanol (Fig. 3c).

Based on this qualitative information the following reaction mechanism was proposed. Methanol dehydrates to dimethyl ether, which reacts further to olefins. The production of dimethyl ether proceeds via the dissociative adsorption of methanol to water and a methoxy group, followed by reaction of this methoxy group with gas-phase methanol to adsorbed dimethyl ether. Propylene and ethylene are the primary gas-phase olefins. The formation of these olefins from dimethyl ether is proposed to proceed via a common intermediate, which can decompose to ethylene or react with adsorbed methanol to propylene and water. Higher olefins are produced via reaction of lighter olefins with methoxy groups on the surface.

5.2. Pump-probe TAP experiments

The oxidation of ethylene over silver powder was mainly studied by pump-probe TAP experiments in order to understand the uniqueness of silver as a selective oxidation catalyst and to discern the roles of different forms of adsorbed oxygen in the mechanism of the total and partial oxidation [25]. In these experiments both ethylene oxide and carbon dioxide were detected as products.

The experiments were performed by pulsing either different amounts of oxygen, as pump molecules, and ethylene, as probe molecules, into the microreactor, at a constant pump-probe time interval and monitoring the CO_2 and ethylene oxide relative yield as a function of the O_2/C_2D_4 ratio (Fig. 4), or constant amounts of reactants at different pump-probe time intervals and monitoring C_2D_4O as a function of the pump-probe interval (Fig. 5).

In the first set of experiments, ethylene oxide production was observed after the injection of ethylene but not after the injection of oxygen, while CO_2 production occurred at both times. The amount of both ethylene oxide and
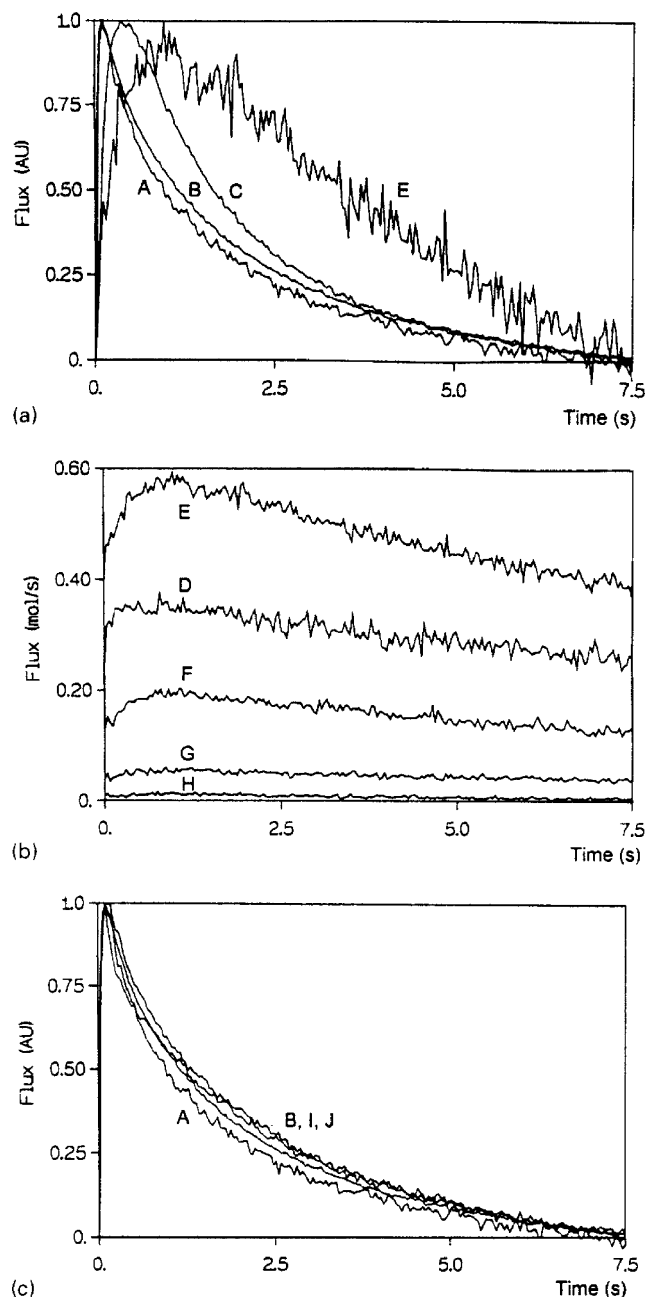

Fig. 3. Normalized (a) and (c) and relative (b) product response observed during a methanol single-pulse experiment with 5.1×10^{15} molecules of methanol per pulse at 775 K over 6 mg H-ZSM-5 zeolite. (A) methanol; (B) water; (C) dimethyl ether; (D) ethylene; (E) propylene; (F) butene; (G) pentene; (H) hexene; (I) methane; (J) formaldehyde [24].

CO_2 formed increases nearly linearly with the size of the oxygen pulse for a O_2/C_2D_4 ratio below 0.6 and becomes nearly independent of the O_2 pulse size for high O_2/C_2D_4 ratios. Moreover, the results of these pump-probe experiments demonstrate that the rate of ethylene oxidation depends on the concentration of adsorbed oxygen and that selective oxidation to ethylene oxide involves the reaction of ethylene with adsorbed oxygen species with no measurable reaction time, as both ethylene and ethylene oxide appear simultaneously at the reactor exit.
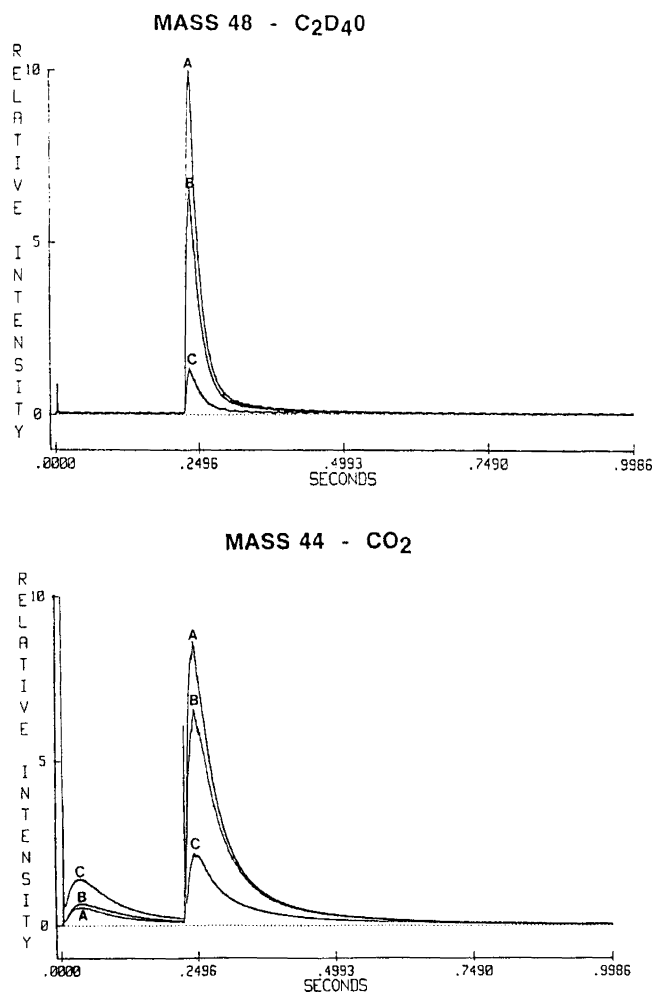
Fig. 4. Series of product curves using O_2 pump and C_2D_4 probe molecules with the relative area ratios of reactants transmitted through the reactor [O_2 to C_2D_4] of (A) 5; (B) 1; (C) 0.5. Injection times are at 0 for O_2 and 0.210 s for C_2D_4 at 523 K catalyst temperature [25].

Fig. 5. Series of C_2D_4O product areas and product curves using O_2 pump and C_2D_4 probe molecules at 523 K catalyst temperature with the following intervals between the O_2 pump and C_2D_4 probe: (A) 20 ms; (B) 50 ms; (C) 72 ms; (D) 117 ms; (E) 425 ms [25].

The second set of pump-probe TAP experiments provides a direct measure of the lifetime of the adsorbed oxygen intermediate. The surface lifetime of active oxygen species was investigated by measuring the C_2D_4O product yield as a function of the pump-probe time interval. The maximum C_2D_4O yield occurred at a large time interval, when the gas-phase oxygen concentration was close to zero, i.e., when the amount of adsorbed oxygen was maximum. This indicates that active oxygen species have a long surface lifetime, which is a result of the role of atomic oxygen on the oxidation process. Actually, the surface lifetime of molecular oxygen is five orders of magnitude less than that of atomic oxygen at 525 K.

5.3. Multipulse TAP experiments

Single-pulse, pump-probe pulse, and multipulse TAP experiments have been performed to obtain information on the mechanism of CO oxidation over very active $Pt/CoO_x/SiO_2$ [26]. We report here only the results obtained from an
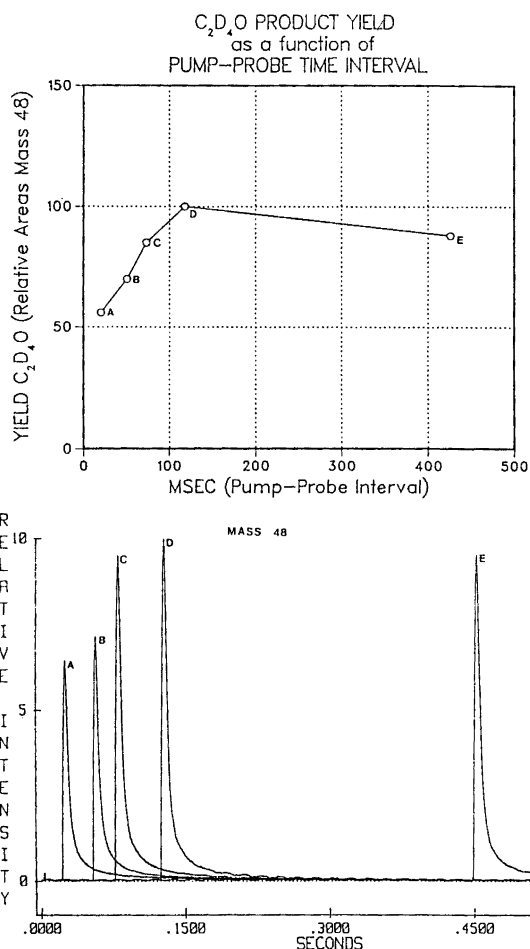
analysis of multipulse TAP experiments. It is known that CO inhibits sites required for the dissociative adsorption of O_2 on Pt. By adding CoO_x, the CO inhibition is expected to become smaller. The CO inhibition effect is well demonstrated in Fig. 6a, where O_2 was pulsed over a CO-precovered Pt/SiO_2 catalyst. O_2 needs a free site to adsorb molecularly and an ensemble of adjacent free sites to dissociate. Due to the slow CO desorption at 327 K, some free sites were generated and the reaction could start. CO_2 desorbed immediately from the Pt surface after its formation providing more free sites for O_2 to dissociate. The CO_2 production increased until a certain value of the CO coverage was reached. From that point the CO_2 formation decreased. On the other hand, when CO was pulsed at 327 K over an oxygen-precovered Pt/SiO_2 catalyst, the reaction started immediately, as shown in Fig. 6b. The oxygen layer provides enough free sites for CO to adsorb and adsorbed CO reacts with atomic oxygen adsorbed on the surface to form CO_2. At higher temperatures (463 K), when CO desorption is fast, the CO inhibition is diminished (Fig. 6c). Moreover, the initially high CO_2 production during the CO pulses over an oxygen-
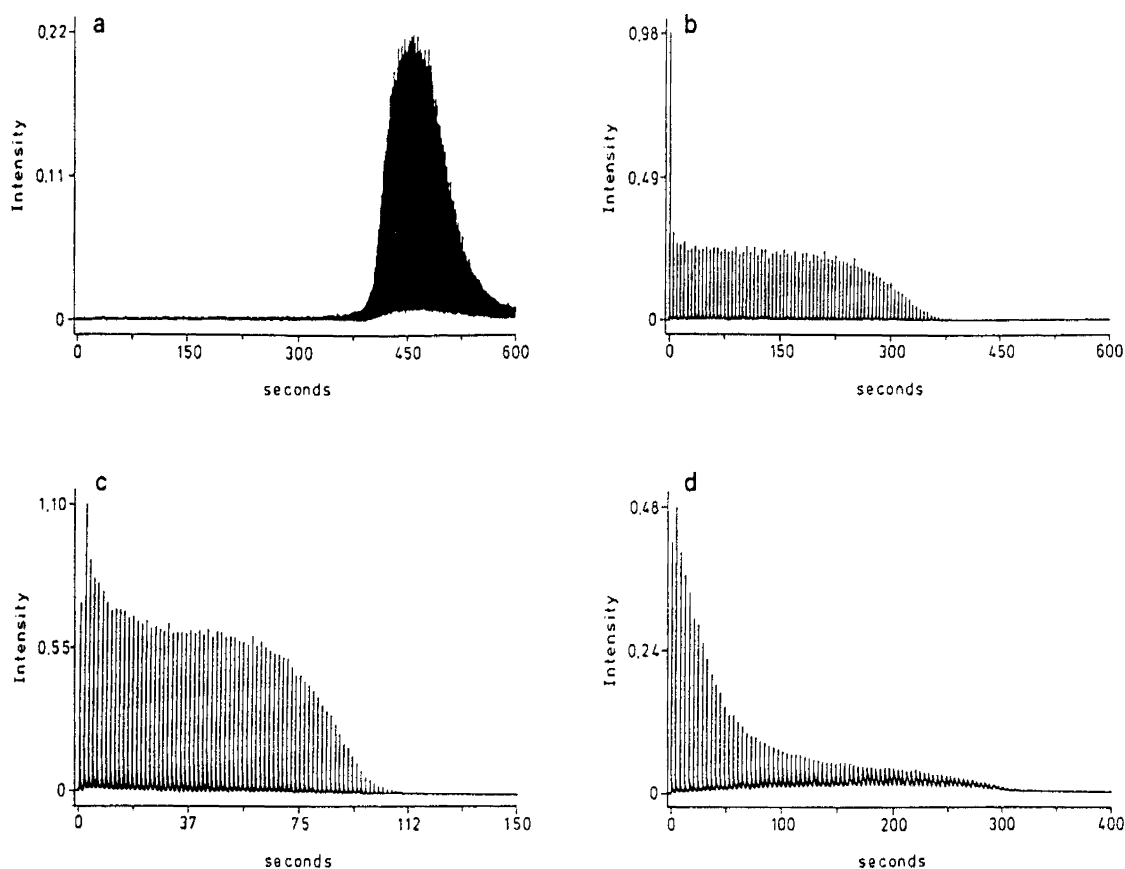
Fig. 6. Multipulse experiments over Pt/SiO$_2$. (a) CO$_2$ signal, measured at 54 °C during O$_2$ pulses over a CO-precovered catalyst; (b) CO$_2$ signal, measured at 54 °C during CO pulses over an oxygen-precovered catalyst; (c) CO$_2$ signal, measured at 190 °C during O$_2$ pulses over the CO-precovered Pt catalyst; (d) CO$_2$ signal, measured at 190 °C during CO pulses over an oxygen-precovered Pt/SiO$_2$ catalyst [26].

precovered Pt/SiO$_2$ catalyst diminished with time due to the fast CO desorption (see Fig. 6d).

Two types of *quantitative information* can be obtained from TAP experiments [27]. The first consists of quantifying the adsorbed amount of certain species on the catalyst surface based on a procedure proposed by Gleaves et al. [1,2]. Such information can be easily obtained by integration of the normalized responses. This procedure has been used, for example, to determine the amount of irreversible adsorbed oxygen on a Au/Ti(OH)$_4^*$ catalyst [28]. The total amount of substance adsorbed in the whole series of pulses is often associated with an estimate for the number of active sites.

The second type of quantitative information involves the determination of reaction rate constants for the elementary reaction steps. This requires setting up a model which describes the transient response of a system. In the TAP experiments, the observed quantities are the outlet flows of gas molecules and related integral quantities, e.g., moments (the mathematical definition for moments is given below). The zeroth moment represents the total amount of gas molecules that emerges from the reactor, and the ratio of the first and the zeroth moments represents the average residence time of gas molecules in the reactor [12,29]. Theoretical studies have been aimed at determining the time dependence of the outlet flow rates and the dependence of

the moments on the reaction–diffusion parameters. Results obtained for different basic models of TAP reactors, which are sets of partial differential equations, are presented below.

6. Quantitative description of TAP experiments by PDEs

The diffusion–reaction processes that occur in TAP pulse response experiments have been described using deterministic models based on PDEs: one-zone model [1,2], two-zone model [9], and three-zone model [2]. A model for the thin-zone configuration and a general multizone model will be discussed in separate sections.

6.1. One-zone reactor

The mathematical framework for the one-zone model was first published in 1988 [1]. The model is based on the following five assumptions:

1. The fractional voidage of the bed is constant.
2. There is no radial gradient of concentration in the catalyst bed.

3. There is neither axial nor radial temperature gradient in the catalyst bed.
4. There is neither intraparticle nor surface diffusion.
5. The diffusivity of each gas is constant, and independent of composition.

The last assumption is the result of using an evacuated microreactor and small pulse intensities that guarantee the validity a Knudsen diffusion regime.

The mass balance equations for a number of important cases are presented below.

6.1.1. Diffusion only

In the Knudsen diffusion regime, the mass balance equation for a nonreacting gas A in a packed bed reactor is given by

$$\varepsilon_b \frac{\partial C_A}{\partial t} = D_{eA} \frac{\partial^2 C_A}{\partial z^2} \qquad (5)$$

with initial condition

$$0 \leqslant z \leqslant L, \qquad t = 0, \qquad C_A = \delta_z \frac{N_{pA}}{\varepsilon_b A} \qquad (6)$$

and boundary conditions

$$z = 0, \qquad \frac{\partial C_A}{\partial z} = 0 \qquad (7)$$

$$z = L, \qquad C_A = 0. \qquad (8)$$

In Eq. (6), the gas concentration is represented by a delta function at the reactor entrance at $t = 0$. Eq. (7) specifies that there is no flux at the reactor entrance when the pulse valve is closed. Eq. (8) results from the fact that the outlet of the reactor is maintained at vacuum conditions, and the concentration of gas at the reactor exit is very close to zero.

The observed characteristics, flow rate, F_A, at the reactor exit are described by

$$F_A = -A D_{eA} \frac{\partial C_A}{\partial z} \bigg|_{z=L}. \qquad (9)$$

There was and still is a debate in the literature about the initial and boundary conditions [30–33]. However, the conditions presented above are reasonably simple and correspond to the simple experimental input set-up. The solutions obtained for these conditions fit rather well with experimental curves. In such a situation, it makes sense to perform catalyst characterization TAP experiments using a set-up corresponding to these conditions. It is useful to express Eq. (5) and initial and boundary conditions (Eqs. (6)–(8)) in a dimensionless form.

Dimensionless axial coordinate:

$$\zeta = \frac{z}{L}. \qquad (10)$$

Dimensionless concentration:

$$\overline{C}_A = \frac{C_A}{N_{PA}/\varepsilon_b AL}. \qquad (11)$$

Dimensionless time:

$$\tau = \frac{t D_{eA}}{\varepsilon_b L^2}. \qquad (12)$$

Written in dimensionless form, Eqs. (5)–(8) are as follows:

$$\frac{\partial \overline{C}_A}{\partial \tau} = \frac{\partial^2 \overline{C}_A}{\partial \zeta^2}. \qquad (13)$$

Initial conditions:

$$0 \leqslant \zeta \leqslant 1, \qquad t = 0, \qquad \overline{C}_A = \delta_\zeta. \qquad (14)$$

Boundary conditions:

$$\zeta = 0, \qquad \frac{\partial \overline{C}_A}{\partial \zeta} = 0, \qquad (15)$$

$$\zeta = 1, \qquad \overline{C}_A = 0. \qquad (16)$$

The solution for the dimensionless concentration, $\overline{C}_A$, can be determined by applying the method of separation of variables

$$\overline{C}_A(\zeta, \tau) = 2 \sum_{n=0}^{\infty} \cos\big((n + 0.5)\pi \zeta\big) \exp\big(-(n + 0.5)^2 \pi^2 \tau\big) \qquad (17)$$

and for the dimensionless flow rate

$$\overline{F}_A(\zeta, \tau) = -\frac{\partial \overline{C}_A(\zeta, \tau)}{\partial \zeta}$$

$$= \pi \sum_{n=0}^{\infty} (2n + 1) \sin\big((n + 0.5)\pi \zeta\big)$$
$$\times \exp\big(-(n + 0.5)^2 \pi^2 \tau\big). \qquad (18)$$

At the exit, where $\zeta = 1$, the dimensionless flow rate can be written as

$$\overline{F}_A = \pi \sum_{n=0}^{\infty} (-1)^n (2n + 1) \exp\big(-(n + 0.5)^2 \pi^2 \tau\big). \qquad (19)$$

Eq. (19) expresses the dimensionless exit flow as a function of dimensionless time. The curve described by Eq. (19) is called the *standard diffusion curve* (SDC) and is plotted in Fig. 7. Obviously, for any TAP pulse response experiment that involves only gas transport, the plot of the dimensionless exit flow rate versus dimensionless time will give the same curve regardless the gas, reactor length, particle size, or reactor temperature. Initial condition Eq. (14) requires that the surface area under the standard diffusion curve be equal to unity. Eq. (19) can be written in dimensional form as

$$\frac{F_A}{N_{pA}} = \frac{D_{eA}\pi}{\varepsilon_b L^2} \sum_{n=0}^{\infty} (-1)^n (2n + 1)$$
$$\times \exp\bigg(-(n + 0.5)^2 \pi^2 \frac{t D_{eA}}{\varepsilon_b L^2}\bigg). \qquad (20)$$

An important property of this dimensional dependence is that its shape is independent on the pulse intensity if the process occurs in the Knudsen regime.
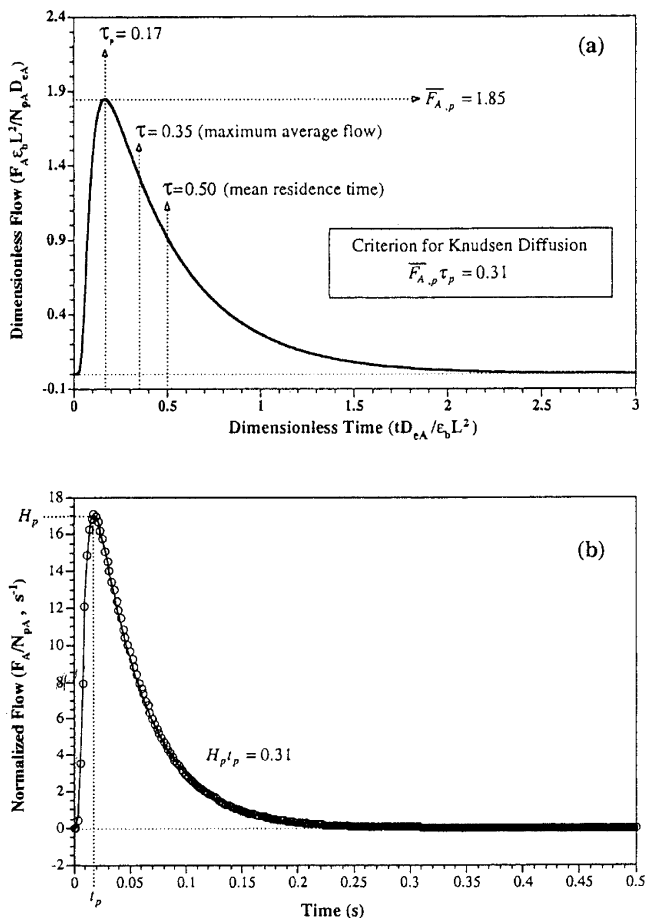
Fig. 7. (a) Standard diffusion curve showing key time characteristics and the criterion for Knudsen diffusion. (b) Comparison of standard curve with experimental inert gas curve over inert packed bed [2].

A unique characteristic of the SDC is the time, τ_p, at which the peak maximum occurs

$$\tau_p = \frac{1}{6} \tag{21}$$

as well as the corresponding height,

$$\overline{F}_{A,p} = 1.85. \tag{22}$$

The corresponding dimensional characteristics, t_p and H_p, will be

$$t_p = \frac{1}{6} \frac{\varepsilon_b L^2}{D_{eA}}, \tag{23}$$

and

$$H_p = 1.85 \frac{D_{eA}}{\varepsilon_b L^2}. \tag{24}$$

Evidently,

$$\overline{F}_{A,p}\tau_p = t_p H_p \approx 0.31. \tag{25}$$

Relationship (25) allows us to verify if an experiment is performed in the Knudsen regime.

The presented criteria for Knudsen diffusion and other properties of SDC have been checked for argon in the TAP system in use at the University of Tokyo [28].

6.1.2. Irreversible adsorption/reaction

One of the most important and the simplest process studied using TAP pulse response experiments is the process of irreversible adsorption (or reaction) combined with Knudsen diffusion. If the adsorption or reaction is characterized by the first-order gaseous concentration dependence, and the change of surface coverage can be neglected due to the small pulse intensity, the mass balance for the gas phase component A can be described by

$$\varepsilon_b \frac{\partial C_A}{\partial \tau} = D_{e,A} \frac{\partial^2 C_A}{\partial z^2} - a_s S_v (1 - \varepsilon_b) k_a C_A. \tag{26}$$

The dimensionless form of Eq. (26) can then be written as

$$\frac{\partial \overline{C}_A}{\partial \tau} = \frac{\partial^2 \overline{C}_A}{\partial \zeta^2} - \bar{k}_a \overline{C}_A, \tag{27}$$

where

$$\bar{k}_a = \frac{a_s S_v (1 - \varepsilon_b) k_a L^2}{D_{e,A}}. \tag{28}$$

The initial and boundary conditions for Eq. (27) are the same as those presented previously for the diffusion only case.

The dimensionless flow at the exit was found to be

$$\overline{F}_A = \pi \exp(-\bar{k}_a \tau) \sum_{n=0}^{\infty} (-1)^n (2n+1) \\ \times \exp(-(n+0.5)^2 \pi^2 \tau). \tag{29}$$

Equation (29) can be also written in dimensional form

$$\frac{F_A}{N_{pA}} = \frac{D_{e,A}\pi}{\varepsilon_b L^2} \exp(-k_a' t) \sum_{n=a}^{\infty} (-1)^n (2n+1) \\ \times \exp\left(-(n+0.5)^2 \pi^2 \frac{D_{e,A}}{\varepsilon_b L^2}\right), \tag{30}$$

where

$$k_a' = \frac{a_s S_v (1 - \varepsilon_b) k_a}{\varepsilon_b}. \tag{31}$$

A comparison of Eq. (30) and SDC Eq. (20) shows that the values of normalized exit flow curve for the diffusion-irreversible adsorption/reaction case are smaller than SDC values by a factor of $\exp(-k_a' t)$. Therefore, the curve of normalized flow for irreversible adsorption/reaction versus time is always placed "inside" the standard diffusion curve. Such a feature can be considered as a "fingerprint" for irreversible adsorption/reaction.

6.1.3. Reversible adsorption

When reversible adsorption occurs, the mass balances become as follows:

For the component A in the gas phase,

$$\varepsilon_b \frac{\partial C_A}{\partial t} = D_{e,A} \frac{\partial^2 C_A}{\partial z^2} - a_s S_v (1 - \varepsilon_b)(k_a C_A - k_d \theta_A). \tag{32}$$

For the component A on the catalyst surface,

$$\frac{\partial \theta_A}{\partial t} = k_a C_A - k_d \theta_A. \tag{33}$$

The dimensionless desorption rate coefficient can be defined as

$$\bar{k}_d = k_d \frac{\varepsilon_b L^2}{D_{e,A}}.$$ (34)

Eqs. (32) and (33) can be transformed into dimensionless form as

$$\frac{\partial \overline{C}_A}{\partial \tau} = \frac{\partial^2 \overline{C}_A}{\partial \zeta^2} - \bar{k}_a \overline{C}_A + \bar{k}_d \overline{\theta}_A,$$ (35)

$$\frac{\partial \overline{\theta}_A}{\partial \tau} = \bar{k}_a \overline{C}_A - \bar{k}_d \overline{\theta}_A,$$ (36)

where

$$\overline{\theta}_A = \alpha \theta_A$$ (37)

and

$$\alpha = (1 - \varepsilon_b) A L \frac{a_s S_v}{N_{pA}}.$$ (38)

Eqs. (35) and (36) can be solved using the initial and boundary conditions presented previously with the additional initial condition for the adsorbed A on the catalyst surface:

$$t = 0, \qquad \overline{\theta}_A = 0.$$ (39)

Solutions for the dimensionless concentration and dimensionless outlet flow can be found in the literature [2]. A particularly interesting feature of the reversible adsorption response is the influence of the kinetic adsorption–desorption parameters on its shape.

In contrast to the case involving irreversible adsorption, the exit flow curve for reversible adsorption will cross the SDC. The intersection of these two curves can be considered as a fingerprint for the reversible adsorption. The point at which the curves intersect depends on the adsorption and desorption rate coefficients.

The reason for such behavior is the delay in molecular transport throughout the reactor caused by the reversible interaction of gas with catalyst.

6.2. Two- and three-zone reactors

The only differences between the models for reactors with two or three zones and the one-zone reactor model are additional boundary conditions between the different zones. For the three-zone reactor, these conditions are described by

$$C_{A,\,\text{zone 1}} \,|\, z_1 = C_{A,\,\text{zone 2}} \,|\, z_1,$$ (40)

$$C_{A,\,\text{zone 2}} \,|\, z_1 = C_{A,\,\text{zone 3}} \,|\, z_2,$$ (41)

$$-D_{eA,\,\text{zone 1}} \frac{\partial C_{A,\,\text{zone 1}}}{\partial z} \bigg|\, z_1 = -D_{eA,\,\text{zone 2}} \frac{\partial C_{A,\,\text{zone 2}}}{\partial z} \bigg|\, z_1,$$ (42)

$$-D_{eA,\,\text{zone 2}} \frac{\partial C_{A,\,\text{zone 2}}}{\partial z} \bigg|\, z_2 = -D_{eA,\,\text{zone 3}} \frac{\partial C_{A,\,\text{zone 3}}}{\partial z} \bigg|\, z_2,$$ (43)

where z_1 is the axial coordinate at the end of zone 1, and z_2 is the axial coordinate at the end of zone 2. Eqs. (40)–(43) describe the continuity of the gaseous concentrations and flows.

7. Moment-based quantitative description of TAP experiments

Another procedure used to distinguish models and estimate kinetic parameters from TAP data is the *moment-based analysis* [12]. Moments as a mathematical tool were introduced in chemical engineering and applied kinetics in the pioneer works of Smith and his followers [34–39].

As mentioned above, the observed TAP data consist of a set of exit flow rates versus time dependencies. It is reasonable, however, to start from the analysis of some integral characteristics (moments) of the exit flow rate because the analytical solutions in integral form can be usually obtained. In fact, these moments reflect the important primary features of the observations in a robust manner.

The moments M_n of exit flow rates (i.e., not of concentrations as usual) are given by

$$M_n = \int_0^t t^n F(t) \, dt.$$ (44)

It is useful to represent moments in dimensionless form as well

$$\bar{m}_n = \int_0^\infty \tau^n \overline{F}_A \, d\tau,$$ (45)

where τ is the dimensionless time

$$\tau = \frac{t}{(\varepsilon_b L^2 / D_{e,A})},$$ (46)

n is the order of the moment, and $\bar{m}_n$ is the dimensionless moment.

In many cases, it is possible to obtain analytical expressions for the moments which contain diffusivity and rate coefficients as parameters. These expressions are not so complicated and can be even simplified performing an experiment in special TAP reactor configurations, such as the thin-zone configuration.

For the reversible reaction, the zeroth dimensionless moment is equal to unity. For irreversible adsorption/reaction it is given by

$$\bar{m}_0 = 1 - X = \frac{1}{\cosh \sqrt{\text{Da}_I}},$$ (47)

where Da_I is the first Damköhler number,

$$\text{Da}_I = \frac{k_a' \varepsilon_b L^2}{D_{e,A}}.$$ (48)

The mean dimensionless residence time for the diffusion only case becomes

$$\tau_{\text{res}} = \frac{M_1}{M_0} = \frac{1}{2}. \tag{49}$$

For irreversible adsorption/reaction, the mean dimensionless residence time is

$$\tau_{\text{res}} = \frac{M_1}{M_0} = \frac{\sum_{n=0}^{\infty} \frac{A(n)}{[B(n)+\text{Da}_{\text{I}}]}}{\sum_{n=0}^{\infty} \frac{A(n)}{B(n)+\text{Da}_{\text{I}}}} \tau_{\text{Dif}}, \tag{50}$$

where

$$A(n) = (-1)^n (2n + 1),$$
$$B(n) = (n + 0.5)^2 \pi^2,$$
$$\tau_{\text{Dif}} = \frac{\varepsilon_{\text{b}} L^2}{D_{\text{e,A}}}.$$

In 1998 [12], another modification, moments as functions of the length were introduced:

$$M = \int_0^{\infty} t^n F(t, x) \, dt. \tag{51}$$

The zeroth moment in this case determines the total number of gas molecules that pass through the given cross section. Using this variable, the typical TAP model represented by the set of partial differential equations can be rewritten as a model in the form of ordinary second-order differential equations, linear and homogeneous.

The analytical solution corresponding to this approach is provided in the literature [39]. In a TAP model the moment rather than the concentration is the independent variable.

8. New theoretical frontiers

8.1. The global transfer matrix equation

Until now, separate theoretical results on determining the time dependence of the outlet flow and the dependence of the moments on the reaction–diffusion parameters have been presented corresponding to the different reactor configurations, but with no unified theoretical framework.

A general and rigorous theory of state-defining experiments for a multizone TAP reactor has been developed [40] using the Laplace transform formalism. The model is a generalization of the three-zone model [2]. In the case of irreversible adsorption/reaction, it is a model with three parameters for the each zone i:

$$\tau_i = \frac{\varepsilon_{\text{b}}^i (\Delta z_i)}{D_{\text{eA}}^i}, \qquad \Psi_i = \sqrt{a_{\text{s}}^i S_{\text{v}}^i k_{\text{ads}}^i (1 - \varepsilon_{\text{b}}^i) \tau_i / \varepsilon_{\text{b}}^i},$$

$$\gamma_i = \frac{D_{\text{eA}}^i}{\Delta z_i}. \tag{52}$$

These characteristics can be interpreted as follows:

– τ_i has dimension time and represents a characteristic time for Knudsen diffusion in a zone;
– Ψ_i is dimensionless and represents a reaction–diffusion parameter for a zone (proportional to $\sqrt{k_{\text{ads}}^i / D_{\text{eA}}^i}$);
– γ_i has the dimension of velocity and represents a characteristic transport conductivity for a zone.

The theory gives explicit expressions for the moments of the outlet flow rate and offers an efficient means to compute the actual profiles of gas and surface concentrations in the reactor and the values of the outlet flow rate numerically using fast Fourier transformation. The central concept of the theory is the global transfer matrix equation, which determines completely the dynamic behavior of the reacting mixture. To describe efficiently the interaction between the m different zones, a Laplace transform technique is used. In this case, every zone will have a unique matrix relating the concentration and flow values at its "left" and "right" boundaries. The concrete form of transfer matrices can be found in the literature [29,40]. Application of the theory to different reactor configurations (one-zone, three-zone, and thin-zone) was facilitated by the use of efficient computer algebra methods.

8.2. Thin-zone configuration

A new type of TAP reactor, the thin-zone TAP reactor (TZTR) has been proposed recently [13]. In this TAP reactor configuration, as mentioned earlier, the thickness of the catalyst zone is made very small compared to the whole length of the reactor. The advantage of this configuration is that change of gaseous concentrations across the catalyst bed can be neglected compared to their average values. Then, the diffusional transport can be explicitly separated from chemical reaction rate.

The active zone reaction rate can be represented by the difference

$$R = F^{\text{left}}(t) - F^{\text{right}}(t) \tag{53}$$

between the diffusional flow values at the boundaries of the thin active zone. This is to some extent analogous to the steady-state CSTR case, in which the reaction rate is also given by a difference of convectional flow rates. For the first-order irreversible adsorption or reaction case, the conversion can be found from the simple expression

$$X = \frac{k_{\text{ads}} \tau_{\text{res,cat}}^{\text{dif}}}{1 + k_{\text{ads}} \tau_{\text{res,cat}}^{\text{dif}}}, \tag{54}$$

$$\tau_{\text{res,cat}}^{\text{dif}} = \varepsilon_{\text{b}} \frac{(\Delta L) L_{\text{II}}}{D_{\text{eA}}}. \tag{55}$$

The dimensionless parameter K_{a} related to the apparent adsorption/reaction rate constant, k_{ads}, as

$$k_{\text{ads}} = K_{\text{a}} \frac{D_{\text{eA}}}{L \, \Delta L \varepsilon_{\text{b}}} \tag{56}$$

can be found from the zeroth moment values:

$$\frac{1}{M_0} = 1 + K_a \frac{L_{II}}{L}.$$

Obviously, expression (54) is analogous to the known relationship for conversion for a first-order reaction in a CSTR that is given by

$$X = \frac{k_{CSTR}\tau_{res}^{conv}}{1 + k_{CSTR}\tau_{res}^{conv}}, \tag{57}$$

where k_{CSTR} is the apparent rate coefficient, τ_{res}^{conv} is the convectional average residence time, and

$$\tau_{res}^{conv} = \frac{V_{cat}}{F_v}. \tag{58}$$

In contrast to τ_{res}^{conv}, $\tau_{res,cat}^{dif}$ is proportional to the position of the catalyst zone in the reactor. In particular, as the catalyst zone is moved closer to the reactor inlet, conversion increases.

Using TZTR, it is possible to determine kinetic parameters of very fast catalytic processes. As an example, the oxidation of propene over oxygen pretreated vanadium-based VPO catalyst is taken [13]. All experiments were conducted using a TAP-2 multifunctional reactor system.

A pulse train of a mixture of propene and argon (90% propene and 10% argon) was injected into the microreactor packed with an oxygen pretreated VPO sample at 653 K. The responses of argon and propene were monitored for a number of pulses to ensure that the pulse intensity remained constant over the pulsing interval. The length of the catalyst zone was kept, 1.7 ± 0.1 mm; the length of the total reactor was 24 mm. The zeroth moments of propene at various positions of the thin zone in the microreactor were calculated using the argon and propene response curves. Fig. 8 shows

the reciprocal of the propene zeroth moment as a function of the catalyst zone position in the reactor.

The dimensionless kinetic parameter K_a was obtained from the slope of the experimental linear dependence ($K_a = 4.49$) and $k_{ads} = 660$ s^{-1} was found using Eq. (56). The possibility of determining such a large rate coefficient confirms the potential of TAP and in particular of the thin-zone configuration.

8.3. Y-procedure

Recently, a special procedure, the so-called Y-procedure, was developed by Yablonsky et al. [22,41] for the analysis of data from the thin-zone TAP experiment. The procedure allows us to determine the gas concentration and reaction rate in the active zone of TZTR.

The mathematical foundation of the Y-procedure is the Laplace-domain analysis. Transposition to the Fourier domain combined with time discretization and filtering of the high-frequency noise leads to an efficient practical method for the reconstruction of gas concentration in a nonsteady-state regime without any presuppositions about the kinetic dependence; i.e., it is a model-free procedure.

Finally, the Y-procedure offers a unique opportunity to relate the temporal evolution of the chemical reaction rate to the surface composition (storage) of the catalyst. Thus, the Y-procedure can be considered as a basis of advanced software for nonsteady-state kinetic data interpretation.

9. Conclusions: what is next?

In heterogeneous catalysis, there are two known kinetic strategies, traditional experiment over industrial multicomponent catalysts under normal conditions (CSTR and PFR, working mostly in a steady-state regime) and surface science experiments under high vacuum conditions mostly over single crystals with well-defined surfaces which are very different from the industrial multicomponent catalyst. Consequently, traditional applied kinetics and surface science kinetics are separated by a "pressure" and "material" gap.

The TAP approach described in this paper can be defined as a "third kinetic strategy," which focuses on the bridging of these "gaps" in the near future. The TAP pulse-response pressure domain (10^{-2}–10^{-1} Pa) is located at the boundary between the traditional applied kinetics and surface science kinetics, and this domain can be extended.

Unlike traditional steady-state experiments, TAP experiments are designed to measure kinetics under dynamic conditions and to obtain a spectrum of parameters corresponding to changes that occur in a catalyst.

Unlike surface science experiments, TAP pulse response experiments can be performed on practical catalytic materials at pressures higher than those used in surface science experiments.
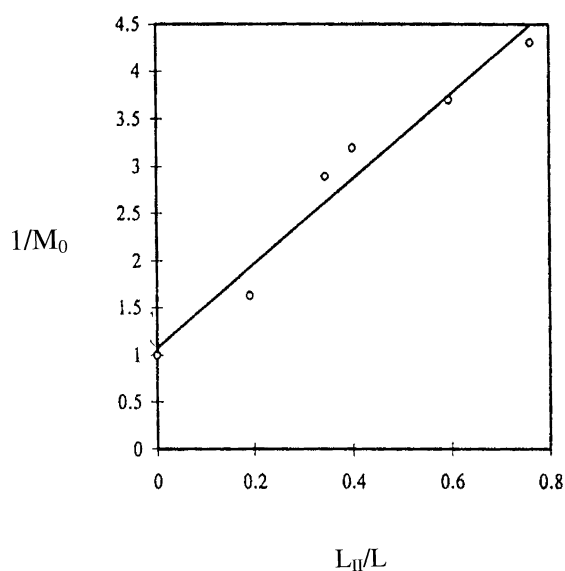
Fig. 8. Reciprocal of the zeroth moment of propene as a function of the position of the catalyst zone in the microreactor. Reaction over oxygen pretreated VPO catalyst at 653 K [13].

A state-altering experiment realized as a multi-pulse TAP experiment will provide both integral (total amounts of consumed/released substances) and differential (kinetic parameters) characteristics at any given catalyst state.

An integral moment-based analysis of the catalytic system insignificantly perturbed during the state-defining experiment will provide the detailed kinetic characterization of the catalyst state and create a basis for formulating the detailed mechanism. In our opinion, this strategy can be efficiently applied for studies of many catalytic reactions, especially selective oxidation of hydrocarbons over multicomponent oxide catalysts.

Acknowledgments

References

[1] J.T. Gleaves, J.R. Ebner, T.C. Kuechler, Catal. Rev. Sci. Eng. 30 (1988) 49.

[2] J.T. Gleaves, G.S. Yablonskii, P. Phanawadee, Y. Schuurman, Appl. Catal. A 160 (1997) 55.

[3] T.A. Nijhuis, L.J.P. VandenBroeke, J.M. VandeGraaf, F. Kapteijn, M. Makkee, J.A. Moulijn, Chem. Eng. Sci. 52 (1997) 3401.

[4] T.A. Nijhuis, L.J.P. van den Broeke, M.J.G. Linders, J.M. van de Graaf, F. Kapteijn, M. Makkee, J.A. Moulijn, Chem. Eng. Sci. 54 (1999) 4423.

[5] J.P. Huinink, J.H.B.J. Hoebink, G.B. Marin, Can. J. Chem. Eng. 74 (1996) 580.

[6] C.O. Bennett, Adv. Catal. 44 (2000) 329.

[7] G. Centi, F. Trifiro, J.R. Ebner, V.M. Franchetti, Chem. Rev. 88 (1988) 55.

[8] F.D. Kopinke, G. Creten, G.F. Froment, Stud. Surf. Sci. Catal. 72 (1992) 317.

[9] B.S. Zou, M.P. Duduković, P.L. Mills, Chem. Eng. Sci. 48 (1993) 2345.

[10] E.P.J. Mallens, J.H.B.J. Hoebink, G.B. Marin, Stud. Surf. Sci. Catal. 81 (1994) 205.

[11] S. Lacombe, H. Zanthoff, C.A. Mirodatos, J. Catal. 155 (1995) 106.

[12] G.S. Yablonsky, S.O. Shekhtman, S. Chen, J.T. Gleaves, Indian Eng. Chem. Res. 37 (1998) 2193.

[13] S.O. Shekhtman, G.S. Yablonsky, J.T. Gleaves, S. Chen, Chem. Eng. Sci. 54 (1999) 4321.

[14] D.G. Huizenga, D.M. Smith, AIChE J. 32 (1986) 1.

[15] A. Brucato, M. Ciofalo, F. Grisafi, R. Tocco, Chem. Eng. Sci. 55 (2000) 291.

[16] C.O. Bennett, AIChE J. 13 (1967) 890.

[17] H. Kobayashi, M. Kobayashi, Catal. Rev. Sci. Eng. 10 (1974) 104.

[18] J. Happel, H.Y. Cheh, M. Otarod, S. Ozawa, A.J. Severdia, T. Yoshida, V. Fthenakis, J. Catal. 75 (1982) 314.

[19] C.O. Bennett, ACS SYM SER. 178 (1982) 1.

[20] P. Bilouen, J. Mol. Catal. 21 (1983) 17.

[21] S.L. Shannon, J.G. Goodwin Jr., Chem. Rev. 95 (1995) 677.

[22] G.S. Yablonsky, S.O. Shekhtman, P. Phanawadee, J.T. Gleaves, Catal. Today 84 (2001) 227.

[23] G.S. Yablonsky, D. Constales, J.T. Gleaves, SAMS, in press.

[24] O. Dewaele, V.L. Geers, G.F. Froment, G.B. Marin, Chem. Eng. Sci. 54 (1999) 4385.

[25] J.T. Gleaves, A.G. Sault, R.J. Madix, J.R. Ebner, J. Catal. 121 (1990) 202.

[26] Y.J. Mergler, J. Hoebink, B.E. Nieuwenhuys, J. Catal. 167 (1997) 305.

[27] S.C. Van der Linde, T.A. Nijhuis, F.H.M. Dekker, F. Kapteijn, J.A. Moulijn, Appl. Catal. A 151 (1997) 27.

[28] M. Olea, M. Kunitake, T. Shido, K. Asakura, Y. Iwasawa, Bull. Chem. Soc. Jpn. 74 (2001) 255.

[29] D. Constales, G.S. Yablonsky, G.B. Marin, J.T. Gleaves, Chem. Eng. Sci. 56 (2001) 133.

[30] G. Creten, D.S. Lafayatis, G.F. Froment, J. Catal. 154 (1995) 151.

[31] B.S. Zou, Doctoral dissertation, Washington University, St. Louis, 1992.

[32] G.V.D. Svoboda, Doctoral dissertation, Washington University, St. Louis, 1992.

[33] J.P. Huinink, Doctoral dissertation, Eindhoven University of Technology, 1995.

[34] M. Suzuki, J.M. Smith, AIChE J. 18 (1972) 326.

[35] N.S. Ragharan, L.K. Doraiswamy, Indian Eng. Chem. Proc. D.D. 16 (1977) 519.

[36] P.A. Ramachandran, J.M. Smith, Indian Eng. Chem. Fundam. 17 (1978) 148.

[37] M.P. Duduković, in: Hugo I. Delasa (Ed.), Chemical Reactor Design and Technology: Overview of the New Developments of Energy and Petrochemical Reactor, Kluwer Academic, Dordrecht/Norwell, MA, 1986, pp. 102–109.

[38] C.Y. Wen, L.T. Fan, Models for Flow Systems and Chemical Reactors, Taiwan, 1975.

[39] R. Aris, Mathematical Theory of Diffusion and Reaction in Permeable Catalysts, Oxford Univ. Press, London, 1975.

[40] D. Constales, G.S. Yablonsky, G.B. Marin, J.T. Gleaves, Chem. Eng. Sci. 56 (2001) 1913.

[41] G.S. Yablonsky, D. Constales, J.T. Gleaves, in: 16th IMACS World Congress on Scientific Computation, Applied Mathematics and Simulation, Lausanne, 2000.